IPP-Report

Max-Planck-Institut
für Plasmaphysik

C.D. Beidler, Ya.I. Kolesnichenko,
V.S. Marchenko, I.N. Sidorenko, and H. Wobig

Stochastic Diffusion of Energetic Ions in Optimized Stellarators

IPP III/265
August 2000

C.D. Beidler, Ya.I. Kolesnichenko,
V.S. Marchenko, I.N. Sidorenko, and H. Wobig

Stochastic Diffusion of Energetic Ions in Optimized Stellarators

IPP III/265
August 2000

Stochastic diffusion of energetic ions in optimized stellarators

C.D. Beidler*, Ya.I. Kolesnichenko**,

V.S. Marchenko**, I.N. Sidorenko*, and H. Wobig*

**Max-Planck-Institut fur Plasmaphysik, EUROATOM Association*

D-85740 Garching bei München, Germany

***Scientific Centre "Institute for Nuclear Research", Kyiv, 03680, Ukraine*

(June 28, 2000)

Abstract

It is shown that the collisionless orbit transformation of the locally trapped and passing particles in the optimized stellarators of the Wendelstein line results in stochastic diffusion of energetic ions. This diffusion can lead to the loss of an essential fraction of energetic ion population from the region where the characteristic diffusion time is small compared to the slowing down time. The loss region and losses can be minimized by shaping the plasma temperature and density profiles so that they satisfy certain requirements. The predictions of the developed theory are in agreement with the results of numerical modelling of confinement of α-particles in a Helias reactor, which was carried out in the work with the use of the orbit following code.

I. INTRODUCTION

It is known that the lack of the axial symmetry in stellarators may result in superbanana orbits of the locally trapped particles. This fact affects transport processes in stellarator plasmas. In particular, it leads to the loss of all locally trapped alpha particles in a conventional stellarators,[1] therefore, a reactor based on such systems is not possible. Several ways are suggested to make the confinement of alpha particles to be acceptable. One of them is to optimize stellarators.[2,3] The optimized stellarators (or Helias, which means HELIcal Advanced Stellarator) are characterized by sufficiently high β (the ratio of plasma pressure to the magnetic field pressure) and concomitant enhanced diamagnetic effects suppressing superbananas. Other suggested ways consist in making such the magnetic configurations that are symmetric in magnetic coordinates (quasi-helical stellarators[4] and quasi-axisymmetric stellarators[5,6]) or are quasi-omnigenous.[7] In all these systems locally trapped particles are to be confined because the contours of the longitudinal adiabatic invariant, $J = \oint v_{||} dl$, are closed and weakly deflect from the magnetic flux surfaces. However, one should expect that there will exist inevitable colissionless losses of alphas in quasi-symmetric and quasi-omnigenous systems because the complete quasi-symmetry and quasi-omnigeneity cannot be achieved. In the present work we will show that a weak point of the optimized stellarators is the presence of the transitioning particles, i.e., particles whose orbits are transformed from the locally trapped to locally passing ones, and vice versa. We will show that a considerable fraction of energetic ions in a Helias configuration can be lost because of the mentioned orbit transformations and concomitant collisionless diffusion.

The physical mechanism responsible for the diffusion of the transitioning particles, which will be studied in this work, consists in the following. The adiabaticity of the particle motion in the phase space breaks down near the separatrix between the regions of the locally trapped and locally passing orbits. Because of this the adiabatic invariant J acquires phase dependent jump each time when a particle crosses the separatrix.[8–10] For successive transitions the phases of the motion do not correlate. Therefore, the multiple

crossings of the separatrix are accompanied by the random walk of particles in the J space, resulting in spatial diffusion.

It should be noted that the stochasticity associated with orbit transitions seems to be observed (but not recognized) in Monte Carlo simulations of fast particle ripple losses in JET and TFTR tokamaks.[11,12] In those simulations the ergodic zone was observed not only in the Goldston-White-Boozer stochastic domain,[13] but also beyond it, close to the midplane of the torus where the ripple wells are formed. The diffusion associated with the orbit transformations of trapped and localized particles in tokamaks was considered in the work[14] where it was shown that resulting loss time for α-particles can be much less than their slowing down time. However, this loss channel plays a minor role in tokamaks where the ripple wells are located only in the narrow band near the midplane and outer circumference of the torus. In contrast to this, in stellarators the local wells occupy the whole plasma cross section. Therefore, one may expect that successive orbit transformations will be an important factor leading to stochasticity and the concomitant loss of energetic ions in the optimized stellarators. A supposition that stochastic diffusion plays an important role in systems with closed contours of J was made in the work by Lotz, et al.[15,16] where confinement of α-particles was studied numerically.

The purpose of the present work is to develop a theory of stochastic diffusion of the energetic ions in the optimized stellarators.

The work is organized as follows. The analysis is carried out in Sec. II. At first, the longitudinal adiabatic invariants of the locally trapped and locally passing particles in terms of the parameters characterizing Helias configurations are calculated. Then the probability of the orbit transformations and a concomitant jump of J are found. Based on them, a coefficient of the collisionless spatial diffusion of energetic particles is obtained. At the end of Sec. II the diffusion coefficient is analyzed and used to evaluate the confinement of the energetic ions in Helias configurations. In Sec. III the confinement of α-particles in a Helias reactor is investigated numerically with a guiding center orbit following code, which extends the analysis by Lotz, et al.[15,16]. In this section the results of numerical calculations are also compared with the predictions of the developed theory. A discussion

and summary of the results obtained in the work are contained in Sec. IV.

II. DIFFUSION OF TRANSITIONING PARTICLES

First of all, we have to specify the magnetic field of the system. We consider a configuration where dominant Fourier harmonics in the magnetic field strength are relevant to a Helias. Namely, we take the magnetic field strength in the form:

$$B = \hat{B}[1 + \epsilon_0(\psi) + \epsilon_m(\psi)\cos N\phi - \epsilon_h(\psi)\cos(\theta - N\phi) - \epsilon_t(\psi)\cos\theta], \tag{1}$$

where ψ, θ, ϕ are the magnetic flux coordinates with ψ the toroidal magnetic flux;[19,20] ϵ_0 describes the change of the vacuum magnetic field due to finite β; ϵ_m, ϵ_h, and ϵ_t are the amplitudes of the mirror, helical, and toroidal harmonics, respectively, ϵ_m being dominant in the plasma core; and $N \gg 1$ is the number of the field periods along the large azimuth of the torus. It is convenient to combine the mirror and helical components in Eq. (1), which leads to

$$B = \hat{B}[1 + \epsilon_0(\psi) + \epsilon_{hm}(\psi,\theta)\cos(N\phi + \chi(\psi,\theta)) - \epsilon_t(\psi)\cos\theta], \tag{2}$$

where

$$\epsilon_{hm}(\psi,\theta) = \left(\epsilon_m^2 + \epsilon_h^2 - 2\epsilon_m\epsilon_h\cos\theta\right)^{1/2}, \qquad \chi(\psi,\theta) = \cos^{-1}\left(\frac{\epsilon_m - \epsilon_h\cos\theta}{\epsilon_{hm}}\right). \tag{3}$$

It follows from Eq. (3) that there exist two characteristic periods in the dependence of B along the field line ($\theta = \iota\phi$, where ι is the rotational transform). The first period, $(\Delta\phi)_1 = 2\pi/\iota$, is due to the toroidal nature of the system (but the helicity essentially contribute to the modulation of B with this period, too); the second one, $(\Delta\phi)_2 \approx 2\pi/N$, is associated with the mirror and helical Fourier components. Because $N \gg 1$, $(\Delta\phi)_2 \ll (\Delta\phi)_1$, which leads to the existence of the local magnetic wells.

We are interested in the particle motion for the time which well exceeds the bounce/transit period, τ_b, associated with the local magnetic wells. In this case, allowing for the fact that a particle weakly deflects from the magnetic field line for τ_b we can use the longitudinal adiabatic invariant J for description of the bounce averaged motion of the

particles. The invariant J has different forms for the locally trapped and locally passing particles.

In particular, for the locally trapped particles, $J^l = \oint v_{||} dl$, (superscript l denotes the locally trapped particles which we will refer to as localized particles). We calculate J^l taking into account Eq. (2) and neglecting the rotational transform and the particle radial excursion (i.e., we take $\psi = \text{const}$, $\theta = \text{const}$). The calculations yield:

$$J^l = J_s(\psi, \theta) f(\kappa^2), \tag{4}$$

where

$$J_s = \frac{16 R_0}{N} \left(\frac{\mu \hat{B} \epsilon_{hm}}{m} \right)^{1/2}, \quad f(\kappa^2) = E(\kappa^2) - (1 - \kappa^2) K(\kappa^2), \tag{5}$$

R_0 is the average radius of the magnetic axis, $K(\kappa)$ and $E(\kappa)$ are the complete elliptic integrals of the first and second kind, respectively, κ is the trapping parameter given by

$$\kappa^2 = \frac{\mathcal{E} - \mu \hat{B}(1 + \epsilon_0 - \epsilon_t \cos\theta - \epsilon_{hm})}{2 \mu \hat{B} \epsilon_{hm}}, \tag{6}$$

$\mathcal{E} = mv^2/2 = \text{const}$ is the particle energy, $\mu = mv_\perp^2/(2B) = \text{const}$ is the particle magnetic moment, and m is the particle mass.

An approximate expression for the longitudional invariant of locally passing particles, J^p, can be obtained by integrating the canonical angular momentum $\mathcal{P} \equiv m v_{||} B_3/B - e\psi_p/c$ ($B_3/B \approx R_0$, B_3 is a covariant component of $\vec{B}$, ψ_p is the poloidal magnetic flux, $d\psi_p/d\psi = \iota$) over the period of the field modulation. Taking again $\psi = \text{const}$, $\theta = \text{const}$ we obtain (c.f.[18]):

$$J^p = \sigma J_s(\psi, \theta) \hat{f}(\kappa^2) - \frac{4\pi e}{mcN} \psi_p, \tag{7}$$

where $\sigma = Sgn\, v_{||}$,

$$\hat{f}(\kappa^2) = k E(1/\kappa^2). \tag{8}$$

Let us consider transitioning particles (i.e., the particles for which $\kappa = 1$ at certain moments, see Fig. 1). Their diffusion arises from the multiple separatrix crossings as a

result of drift-induced slow modulations of $\epsilon_{hm}(\psi,\theta)$ and $\chi(\psi,\theta)$. Modulation of $\chi(\psi,\theta)$ corresponds to the slow change of the local well position along the trajectory of passing particles and results in $p^+ \leftrightarrow p^-$ transitions (p^+ and p^- are passing particles with $v_{||} > 0$ and $v_{||} < 0$, respectively) without the change of the orbit topology. Hereafter we ignore the contribution from such crossings, and consider only $p \leftrightarrow l$ transitions associated with the modulation of the local well depth $\epsilon_{hm}(\psi,\theta)$.

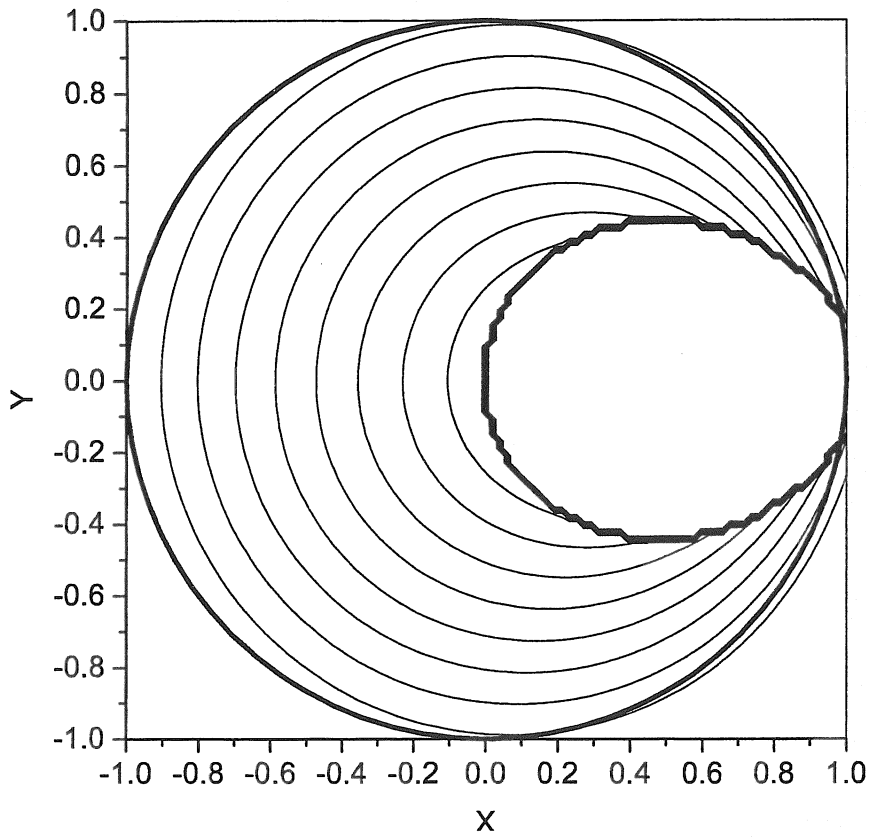

Fig.1. Sketch of level contours of J for the locally trapped particles (thin lines) and the $\kappa = 1$ contour (bold line inside the plasma) in a Helias. Locally trapped particles moving along the $J = const$ contours become locally passing ones after crossing the bold line.

The corresponding diffusion coefficient can be defined as follows:

$$D = \frac{\langle (\Delta r)^2 \rangle}{\tau}, \tag{9}$$

where Δr is the change of the particle radial coordinate caused by the orbit transformation, r being the effective flux surface radius defined by the equation $\psi = \hat{B} r^2/2$; τ is the characteristic time,

$$\tau = \frac{1}{2}(\tau^l + \tau^p), \tag{10}$$

τ^l and τ^p being the characteristic times of the motion of a particle in the localized and passing states. The factor 1/2 takes into account that a particle crosses the separatrix twice per full period of the hybrid passing-localized orbit. The time τ^l is essentially the precession time of a localized particle given by

$$(\tau^l)^{-1} = -\frac{c}{2\pi e(\partial J^l/\partial \mathcal{E})} \frac{\partial J^l}{\partial \psi}. \tag{11}$$

The equation (11) yields:

$$(\tau^l)^{-1} = \frac{\mathcal{E}\hat{B}}{2\pi m \omega_B} \left(\epsilon_0' - \epsilon_t' \cos\theta + \frac{\epsilon_h'}{\epsilon_{hm}} (\epsilon_h - \epsilon_m \cos\theta) \right). \tag{12}$$

where prime denotes derivative over ψ.

One can see that $(\tau^p)^{-1}$ is proportional to the poloidal velocity of a passing particle, $d\theta^p/dt$, and the probability for this particle to be trapped into the local magnetic well, P. Therefore, we write:

$$(\tau^p)^{-1} = \frac{P}{2\pi} \frac{d\theta^p}{dt}. \tag{13}$$

To calculate P we use the following expression:[21]

$$P = \left. \frac{dJ^l/dt}{dJ^p/dt} \right|_{\kappa^2=1}. \tag{14}$$

Taking into account Eq. (4) and that $dJ_s/dt|_{\kappa^2=1} = 0$ we present the numerator of Eq. (14) as follows:

$$\left. \frac{dJ^l}{dt} \right|_{\kappa^2=1} = J_s \left. \frac{\partial f}{\partial \kappa^2} \frac{d\kappa^2}{dt} \right|_{\kappa^2=1}. \tag{15}$$

Using the equations of bounce averaged motion of the localized particles,

$$\frac{d\psi}{dt} = \frac{c}{e\partial J/\partial \mathcal{E}}\frac{\partial J}{\partial \theta}, \quad \frac{d\theta}{dt} = -\frac{c}{e\partial J/\partial \mathcal{E}}\frac{\partial J}{\partial \psi}, \tag{16}$$

we obtain:

$$\frac{d\kappa^2}{dt} = \frac{\partial \kappa^2}{\partial \psi}\frac{d\psi^l}{dt} + \frac{\partial \kappa^2}{\partial \theta}\frac{d\theta^l}{dt} = \frac{c}{e}\mathcal{D}(\psi,\theta)\frac{1}{\partial J^l/\partial \mathcal{E}}, \tag{17}$$

where

$$\mathcal{D}(\psi,\theta) \equiv \frac{\partial J_s}{\partial \theta}\frac{\partial \kappa^2}{\partial \psi} - \frac{\partial J_s}{\partial \psi}\frac{\partial \kappa^2}{\partial \theta}. \tag{18}$$

On the separatrix, which is determined by the equation $\kappa^2(\psi_s,\theta_s) = 1$, we have (a term with derivative $d\epsilon_m/d\psi$ is neglected, and subscript "s" is omitted):

$$\left.\frac{\partial \kappa^2}{\partial \psi}\right|_{\kappa^2=1} = \frac{1}{2\epsilon_{hm}}\left[\epsilon_t' \cos\theta - \epsilon_0' - \frac{\epsilon_h'}{\epsilon_{hm}}(\epsilon_h - \epsilon_m \cos\theta)\right], \tag{19}$$

$$\left.\frac{\partial \kappa^2}{\partial \theta}\right|_{\kappa^2=1} = -\frac{\sin\theta}{2\epsilon_{hm}}\left(\frac{\epsilon_h\epsilon_m}{\epsilon_{hm}} + \epsilon_t\right), \tag{20}$$

$$\frac{\partial J_s}{\partial \psi} = \frac{16R_0}{N}\left(\frac{\mu\hat{B}\epsilon_{hm}}{m}\right)^{1/2}\frac{\epsilon_h'}{2\epsilon_{hm}}\frac{\epsilon_h - \epsilon_m\cos\theta}{\epsilon_{hm}}, \quad \frac{\partial J_s}{\partial \theta} = \frac{16R_0}{N}\left(\frac{\mu\hat{B}\epsilon_{hm}}{m}\right)^{1/2}\frac{\epsilon_h\epsilon_m}{2\epsilon_{hm}^2}\sin\theta, \tag{21}$$

$$\mathcal{D}(\psi,\theta)|_{\kappa^2=1} = -\frac{4R_0}{N}\left(\frac{\mu\hat{B}}{m}\right)^{1/2}\frac{\delta}{\epsilon_{hm}^{5/2}}\sin\theta, \tag{22}$$

$$\delta \equiv \epsilon_h\epsilon_m\epsilon_0' - \epsilon_h'(\epsilon_h - \epsilon_m\cos\theta)\epsilon_t - \epsilon_h\epsilon_m\epsilon_t'\cos\theta, \tag{23}$$

Calculating the denominator in Eq. (14), we take into account that $d\psi/dt|_{\kappa^2=1} = 0$ and that the second term in Eq. (7) dominates. Then we obtain:

$$\left.\frac{dJ^p}{dt}\right|_{\kappa^2=1} \approx -\frac{\sigma c J_s}{e(\partial J^p/\partial \mathcal{E})}\frac{\partial J^p}{\partial \psi}\frac{\partial \hat{f}}{\partial \kappa^2}\frac{\partial \kappa^2}{\partial \theta} = \frac{4\pi v^2}{N}\epsilon_{hm}\left.\frac{\partial \kappa^2}{\partial \theta}\right|_{\kappa^2=1}, \tag{24}$$

where $\partial\kappa^2/\partial\theta|_{\kappa^2=1}$ is given by Eq. (20).

The obtained relations enable us to write the probability of the orbit transformations given by Eq. (14) as

$$P = \frac{2\hat{B}R_0}{\pi\omega_B}\left(\frac{\mu\hat{B}\epsilon_{hm}}{m}\right)^{1/2}\frac{\delta}{\epsilon_h\epsilon_m + \epsilon_t\epsilon_{hm}}, \tag{25}$$

where $\omega_B = e\hat{B}/(mc)$. Combining Eqs. (25), (13) we have:

$$(\tau^p)^{-1} = -\frac{cP}{2\pi e(\partial J^p/\partial\mathcal{E})}\frac{\partial J^p}{\partial\psi} = \frac{\mathcal{E}\hat{B}}{2\pi m\omega_B}\frac{\delta}{\epsilon_h\epsilon_m + \epsilon_{hm}\epsilon_t}. \tag{26}$$

Comparing Eq. (26) with Eq. (12) we conclude that typically the times which a transitioning particle spend on each part of the hybrid trajectory are almost equal.

Let us calculate now the change of the adiabatic invariant caused by separatrix crossing. We proceed from the following expression:[8–10]

$$\Delta J = -\frac{1}{\omega}\frac{dJ_s^l}{dt}\Lambda(\xi_s), \tag{27}$$

where $\omega = 2K(\kappa)(m\partial J^l/\partial\mathcal{E})^{-1}/\pi$, $\Lambda(\xi_s) = \ln[2\sin(\pi\xi_s)]$, and ξ_s is a crossing parameter which can be expressed in terms of the coordinate ϕ_s of the point where the trajectory crosses the separatrix as $\xi_s = 0.5\,(1 - \sin N\phi_s/2)$ with $-\pi/N \leq \phi_s \leq \pi/N$.

When multiple trapping occurs, ξ_s can be regarded as a random value uniformly distributed in the interval $(0, 1)$. Then we obtain:

$$< \Delta J >= 0, \qquad < (\Delta J)^2 >= \frac{\pi^2}{12}\left(\frac{1}{\omega}\frac{dJ_s^l}{dt}\right)^2. \tag{28}$$

The corresponding radial jump can be found from the relation:

$$\Delta\psi = \Delta J\frac{\partial\psi}{\partial J^l}, \tag{29}$$

where ψ is to be taken at the transition point determined by the equation

$$J_s(\psi, \theta(\psi)) = J^l(\psi, \theta, \alpha), \tag{30}$$

and $\alpha \equiv \mathcal{E}/\mu\hat{B} - 1$ is a pitch angle variable. From Eq. (30) we find:

$$\frac{\partial\psi}{\partial J^l} = \left(\frac{\partial J_s}{\partial\psi} + \frac{\partial\theta}{\partial\psi}\frac{\partial J_s}{\partial\theta}\right)^{-1} \tag{31}$$

with $\partial\theta/\partial\psi$ determined by the particle trajectory. The latter, as it follows from Eq. (16), is determined by the following equation:

$$\frac{\partial\theta}{\partial\psi} = -\frac{\partial J^l/\partial\psi}{\partial J^l/\partial\theta}. \tag{32}$$

Substituting Eq. (32) to Eq. (31) we obtain:

$$\frac{\partial\psi}{\partial J^l} = \frac{(\partial\kappa^2/\partial\theta)|_{\kappa^2=1}}{\mathcal{D}(\psi,\theta)}. \tag{33}$$

Using Eqs. (4), (15)-(18), the jump of the adiabatic invariant given by Eq. (27) can be presented in the form:

$$\Delta J = \frac{\pi cm}{2eK(\kappa)} J_s \frac{\partial f}{\partial\kappa^2}\mathcal{D}(\psi,\theta)\Lambda(\xi_s) = \frac{\pi}{4}\frac{B_0}{\omega_c} J_s \mathcal{D}(\psi,\theta)\Lambda(\xi_s). \tag{34}$$

This expression together with Eqs. (29), (33) and the relation $\psi = \hat{B}r^2/2$ yield:

$$\Delta r = \frac{\pi}{4}\frac{J_s}{\omega_B r}\left.\frac{\partial\kappa^2}{\partial\theta}\right|_{\kappa^2=1}\Lambda(\xi_s). \tag{35}$$

Combining Eqs. (13), (25), (35), and (9) we finally obtain:

$$D = \frac{\pi^3}{12}\frac{R_0^2\,\omega_B\rho_B^4}{N^2 a r^3}\frac{\delta}{\epsilon_{hm}^3}\frac{(\epsilon_h\epsilon_m + \epsilon_t\epsilon_{hm})^2}{(\epsilon_h\epsilon_m + \epsilon_{hm}\epsilon_t + \delta/\delta_1)}\sin^2\theta, \tag{36}$$

where $\rho_B = (2\mathcal{E}/m)^{1/2}/\omega_B$ is the Larmor radius, $\epsilon_{hm} \equiv \epsilon_{hm}(r,\theta)$,

$$\delta \equiv \delta(r,\theta) = \epsilon_h\epsilon_m\epsilon'_{0x} - (\epsilon_h - \epsilon_m\cos\theta)\epsilon_t\epsilon'_{hx} - \epsilon_h\epsilon_m\epsilon'_{tx}\cos\theta, \tag{37}$$

$$\delta_1 \equiv \epsilon'_{0x} + \frac{\epsilon'_{hx}}{\epsilon_{hm}}(\epsilon_h - \epsilon_m\cos\theta) - \epsilon'_t\cos\theta, \tag{38}$$

$x = r/a$, $\epsilon'_{jx} \equiv d\epsilon_{jx}/dx$, $j = h,m,t$; $\theta \equiv \theta(r,\alpha)$ is the poloidal angle at a point of $t \to l$ transition (see Fig. 1), which is determined by the following expression ($\kappa^2 = 1$):

$$\cos(\theta(r,\alpha)) = \frac{1}{\epsilon_t}\left[\epsilon_0 - \alpha - \frac{\epsilon_h\epsilon_m}{\epsilon_t} + \sqrt{\left(\epsilon_0 - \alpha - \frac{\epsilon_h\epsilon_m}{\epsilon_t}\right)^2 + \epsilon_h^2 + \epsilon_m^2 - (\alpha - \epsilon_0)^2}\right], \tag{39}$$

$\alpha_{min} \le \alpha \le \alpha_{max}$, $\alpha_{min} = \epsilon_m - \epsilon_h - \epsilon_t + \epsilon_0$, $\alpha_{max} = \epsilon_m + \epsilon_h + \epsilon_t + \epsilon_0$. When $\epsilon_t \ll \epsilon_h \ll \epsilon_m$, which is the case in the plasma core of a Helias, the maximum diffusion coefficient can be evaluated as

$$D_{max} \approx \frac{4}{\pi}\frac{R^2\omega_B\rho^4}{N^2 a r^3}\frac{\epsilon_h^2}{\epsilon_m}\epsilon'_0. \tag{40}$$

The condition that an energetic ion will be lost because of diffusion (rather then displaced within the plasma) is $\tau_d \ll \tau_s$, where τ_s is a characteristic slowing down time of this ion, and τ_d is its confinement time,

$$\tau_d(r) \sim \frac{(a-r)^2}{D}. \tag{41}$$

Because the diffusion coefficient given by Eq. (36) strongly grows with the particle energy, this condition must be well satisfied for a particle escaping to the wall. Taking this into account, we introduce a critical radius, r_{crit}, such that when $r \geq r_{crit}$, the transitioning particles are lost before they will be thermalized. The radius r_{crit} can be defined as a solution of the equation $S\tau_d = \tau_s$ where $S \sim 3$.

The fraction of transitioning particles at a given flux surface, which is essentially the loss fraction of α-particles when $S \geq 3$, can be estimated using Eq. (39) as follows:

$$\nu \approx \frac{1}{1+\alpha_{min}} - \frac{1}{1+\alpha_{max}} = \frac{2(\epsilon_h + \epsilon_t)}{(1+\epsilon_m+\epsilon_0)^2 - (\epsilon_h+\epsilon_t)^2}. \tag{42}$$

Let us evaluate τ_d and ν of α-particles in a Helias reactor with $N = 5$, $R_0/a = 10$, and $\langle\beta\rangle = 5\%$[17]. At first, we make a simple estimate by approximating Fourier harmonics of the magnetic field as follows:

$$\epsilon_m = 0.1, \quad \epsilon_0 = 0.08x^2, \quad \epsilon_t \simeq 0.05x, \quad \epsilon_h = 0.08x. \tag{43}$$

Then at $r = a/2$ we find:

$$\tau_d(a/2) \approx \frac{5}{\omega_B}\left(\frac{a}{\rho_B}\right)^4, \quad \nu(a/2) \sim 10\%. \tag{44}$$

Assuming $B = 5T$ and using Eq. (44) we obtain $\tau_d \approx 0.02s$ for $a/\rho_B = 30$, and $\tau_d \approx 0.06s$ for $a/\rho_B = 40$. On the other hand, the slowing down time of a $3.5MeV$ alpha particle in a plasma with the electron density $n_e = 2 \div 3 \times 10^{20} m^{-3}$, and the temperature $T = 10 \div 15keV$ is $\tau_s \sim 0.1sec$. This means that an essential fraction of alphas will be lost to the wall from a flux surface with the radius $r/a = 0.5$ in a system with $a/\rho_B = 30$, but particles can hardly escape from the $r/a = 0.5$ surface when $a/\rho_B = 40$. Furthermore, if profile shapes of the plasma density and temperature change in a way that τ_s strongly

decreases with the radius, the condition $\tau_d \ll \tau_s$ will violate near the plasma edge. Then energetic ions will diffuse to the periphery and thermalized in that region. In this case the main effect of the stochastic diffusion will be the broadening of the radial profile of the power deposition of energetic ions rather than their loss. As $\tau_s \propto T^{3/2}/n_e$, this will be the case when the temperature strongly decreases with r, whereas the $n_e(r)$ profile is flat.

To obtain a general picture and to verify these estimates we calculated D and τ_d as the function of r using exact Fourier harmonics , see Figs. 2-6. We observe that Eq. (44) represents a reasonable approximation.

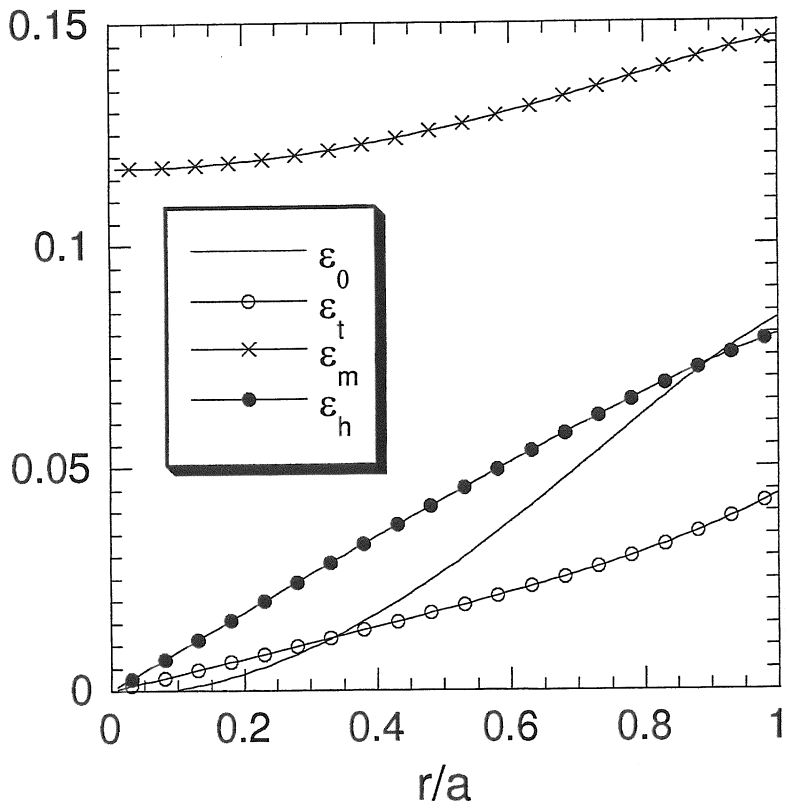

Fig.2. Fourier harmonics of the magnetic field strength in a Helias reactor and the high-mirror high-ι variant of Wendelstein 7-X with $\langle\beta\rangle = 4.7\%$

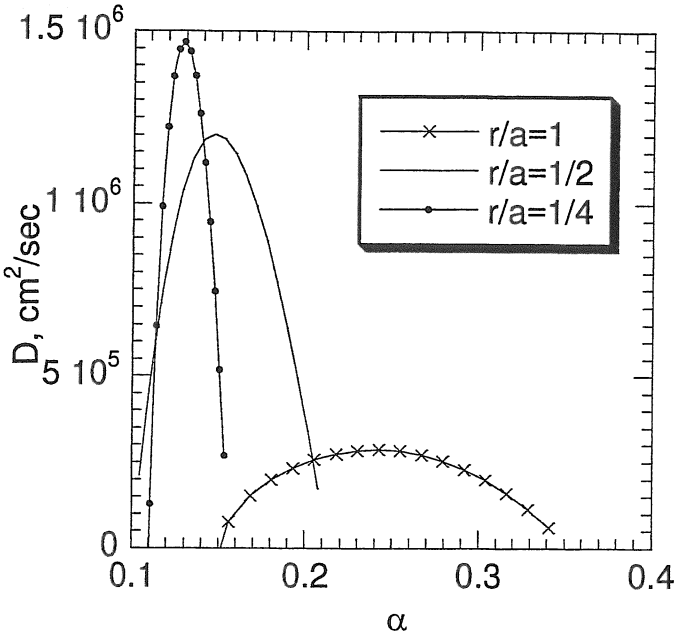

Fig.3. Diffusion coefficient versus the pitch parameter $\alpha \equiv \mathcal{E}/\mu B - 1$ *for various* r/a. *The following parameters were used:* $\langle\beta\rangle = 4.7\%$, $a/\rho_B = 30$, $B = 4.75T$.

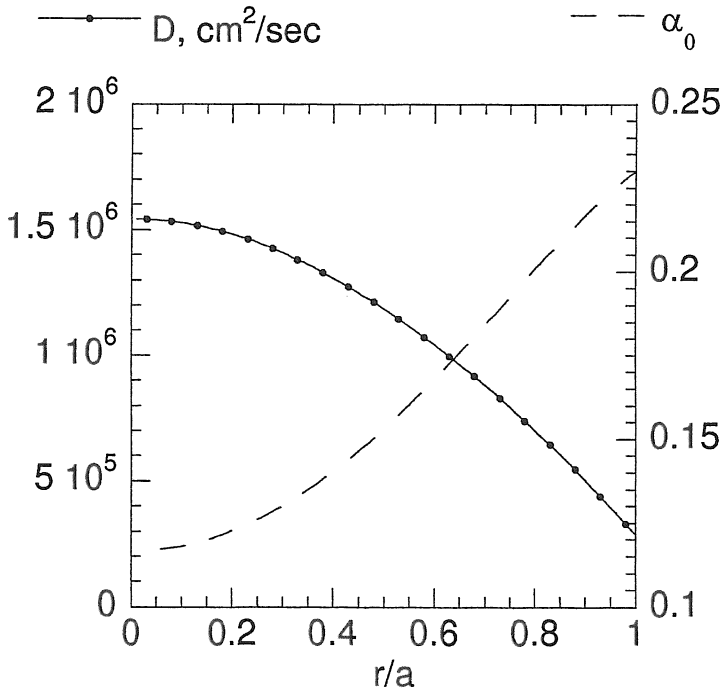

Fig.4. Radial dependence of the diffusion coefficient and $\alpha_0 = (\alpha_{max} + \alpha_{min})/2$ *for the same parameters as in Fig. 3. The used magnitudes of* α *are shown by the dashed line.*

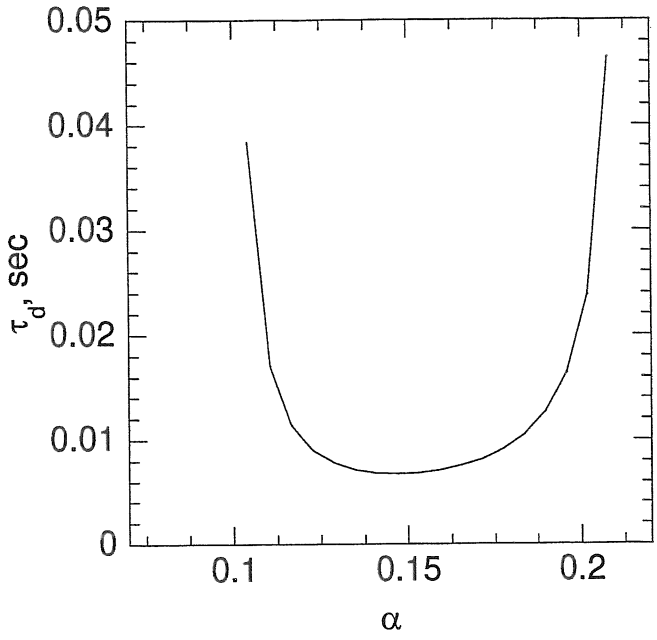

Fig.5. The diffusion time versus α for the Fourier harmonics of the magnetic field shown in Fig. 2.

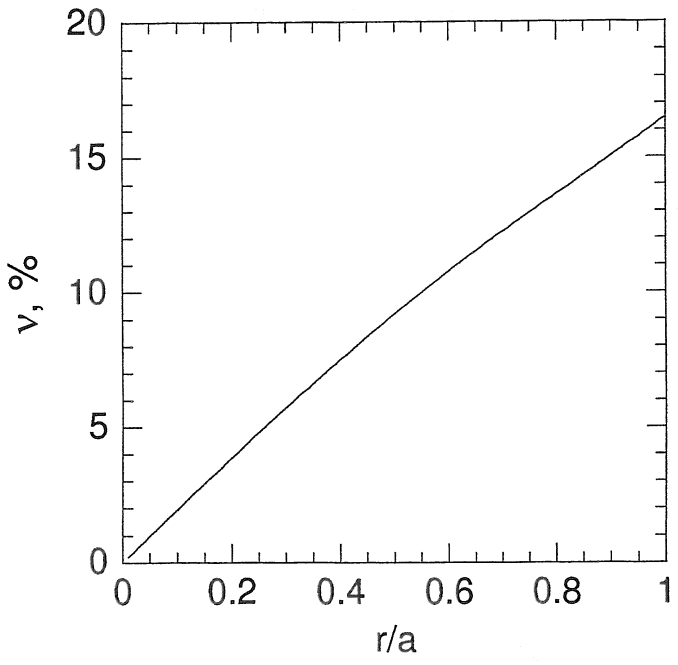

Fig.6. Fraction of transitioning particles versus r for the same parameters as in Fig. 3.

III. NUMERICAL MODELLING OF ALPHA PARTICLE CONFINEMENT IN A HELIAS REACTOR

Numerical integration of the guiding center equations of motion has been used in the past to investigate α-particle confinement in Helias configurations.[15,16] It was found that when Coulomb collisions are neglected in a simulation with $<\beta> \approx 0.05$ and $a/\rho_B = 30$, that approximately 10% of α-particles launched from the $r/a \approx 1/3$ flux surface were lost from the plasma and that the confinement time of such lost particles satisfied $\tau_d \geq 0.03\ s$.[15] Both of these results are in good agreement with the estimates provided above. Repeating the numerical simulations including collisional effects (slowing down and pitch-angle scattering), α-particle losses were found to occur after $0.01\,s$ and a significant fraction of the energy loss observed in the simulation was due to escaping particles with energies greater than 1 MeV.[16]

For the present work, similar calculations have been undertaken for a Helias reactor[17] with $R_0 = 22\ m$, $a = 1.8\ m$ and $B_0 = 4.75\ T$ (and thus $a/\rho_B = 31.5$). The plasma parameters and profiles are taken from 1–D numerical simulations for two scenarios:

- a high-density (central electron density $n_e(0) = 3 \times 10^{20}\ m^{-3}$), low-temperature (central temperature $T(0) = 15\ keV$) case similar to that considered previously,[15,16] and
- a low-density ($n_e(0) = 1.5 \times 10^{20}\ m^{-3}$), high-temperature ($T(0) = 25\ keV$) case.

These profiles are illustrated in Fig. 7. Also shown are the α-particle birth profiles which result therefrom, in the form of cumulative probability curves (i.e. the likelihood that an α-particle is born at a value of normalized radius less than a given x). For simplicity, it has been assumed that the densities of deuterium and tritium are equal and given be $n_e/2$ and that the temperatures of all species are identical.

The simulations described here begin with an ensemble of 250 α-particles, all of which have the same initial energy $\mathcal{E}_0 = 3.52\ MeV$ but are assigned to different starting radii according to the appropriate birth profile; the remaining spatial and velocity coordinates are chosen randomly. The guiding center trajectory of each α-particle is then followed

in the magnetic field of the Helias reactor determined by an equilibrium code for $<\beta>$ = 0.047. The particles undergo slowing down and pitch-angle scattering on the local background plasma. An α-particle is considered lost if it reaches $x = 1$. When this occurs its energy, $\mathcal{E}_{loss}$, and confinement time, τ_{loss}, are recorded and it is removed from the simulation without replacement. All α-particles which remain confined are followed until the sum of their energies is reduced to 88 MeV (10% of the total energy which the 250 simulation particles initially possessed). This typically implies a simulation time roughly equal to $\tau_s(x = 0)$.

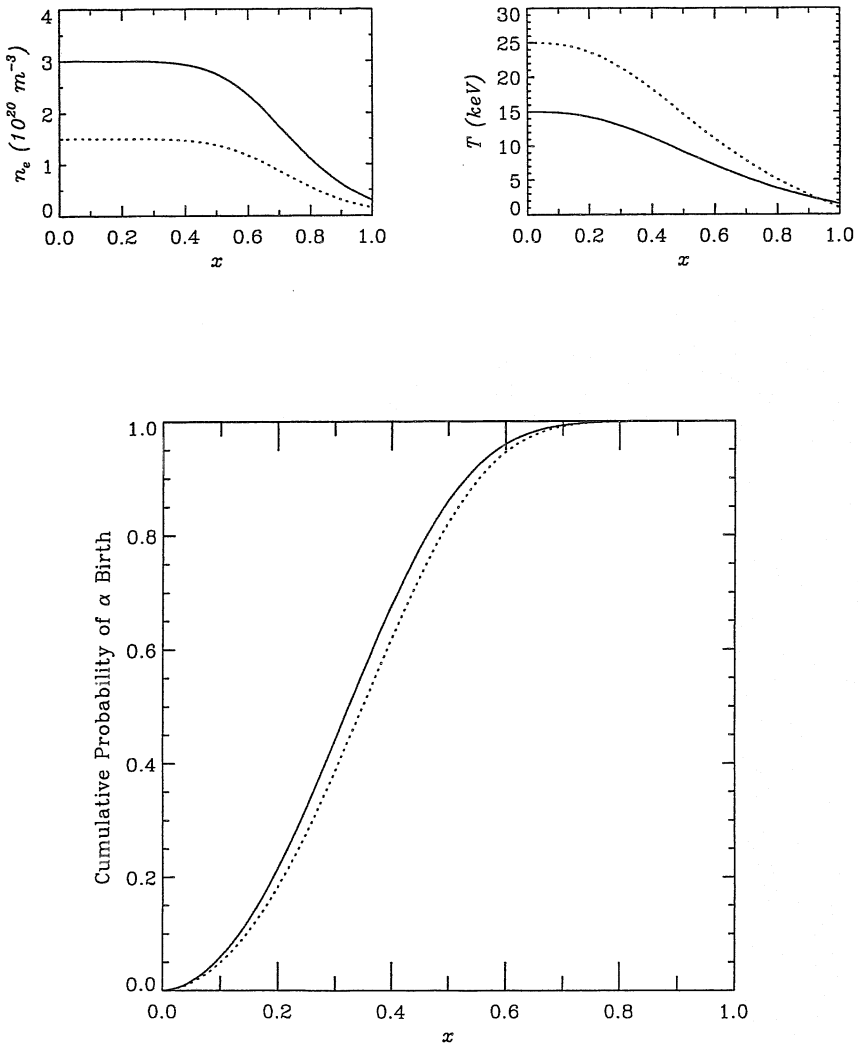

Fig.7. Density and temperature profiles used for the high-n, low-T (solid line) and low-n, high-T (dotted line) scenarios. Also shown are the corresponding α-particle birth profiles as cumulative probability curves.

The two scenarios considered here lead to nearly identical birth profiles for the α-particles (Fig. 7) but slowing-down times which differ by a factor of four. Given the arguments of the previous section, one must therefore expect greater losses of fast α-particles for the low-density, high-temperature scenario as even those particles born near the plasma center (with $\tau_s \approx 0.46$ s) can diffuse to the plasma edge before slowing down. These expectations are borne out by the results of the numerical simulations which are presented in Fig. 8 (high-n, low-T scenario) and in Fig. 9 (low-n, high-T scenario). Here, the fraction of initial energy transferred to the background plasma, $\Delta\mathcal{E} \equiv 1 - \mathcal{E}_{loss}/\mathcal{E}_0$, and the birth radius, x_0 are plotted versus τ_{loss} for all particles lost in the course of the simulation.

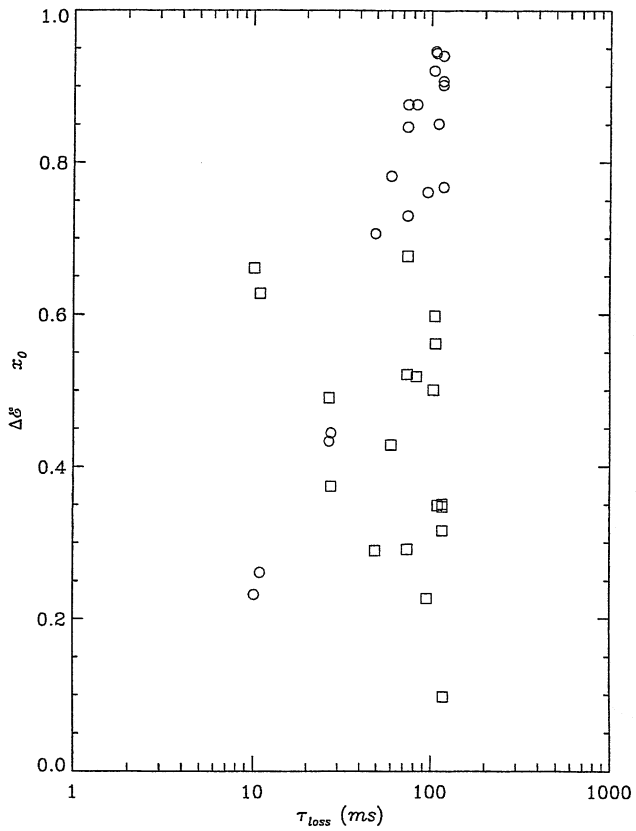

Fig.8. The fraction of initial energy transferred to the background plasma before its escape, $\Delta\mathcal{E}$, is plotted as a function of confinement time, τ_{loss}, (symbol: ○) for each of the 19 α-particles lost during the 0.12 s of the high-n, low-T simulation. Also shown is the normalized radius at which the particle began the simulation, x_0 (symbol: □)

The relevant statistical data may be briefly summarized as follows :

- For the high-n, low-T scenario 19 particles are lost during a simulation time of 0.12 s leading to a lost-energy fraction of 0.02, 60% of which is due to 5 particles with $\mathcal{E}_{loss} >$ 1 MeV.
- In the low-n, high-T scenario losses increase to 54 particles during a simulation time of 0.44 s. The lost-energy fraction is 0.09, of which 85% can be attributed to 32 particles with $\mathcal{E}_{loss} > 1$ MeV.

The effects of a broader density profile were also investigated for the high-density, low-temperature scenario by setting $n_e(a)/n_e(0) = 1/3$; the temperature profile was left unchanged. No statistically significant differences were observed in the numerical simulation, however, as the higher edge density leads not only to more effective slowing down in the plasma periphery but also to a broader birth profile of α-particles and these two effects largely counteract one another.

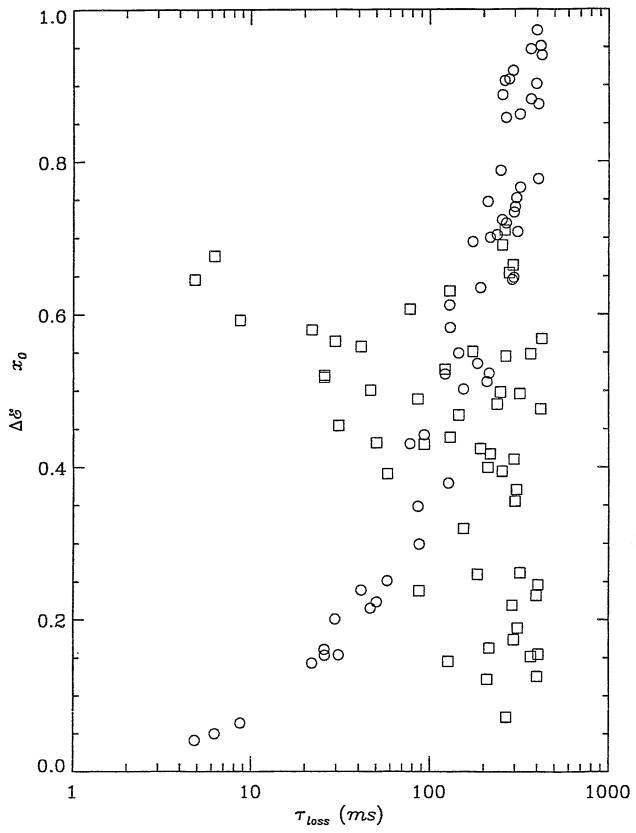

Fig.9. As in Fig. 8 for the 54 α-particles lost during the 0.44 s of the low-n, high-T simulation

IV. SUMMARY AND CONCLUSIONS

The theory developed in the present work shows that transitioning energetic particles in advanced stellarators of Wendelstein line undergo the stochastic diffusion associated with the orbit transformation of the localized and passing particles. This diffusion may lead to the loss of α-particles and other energetic ions from the plasma core of the Helias reactor[17] and Wendelstein 7-X[22] for the time $\geq 0.01s$. The fraction of escaping α-particles can be rather large. It is about 10% for α-particles produced at $r \sim a/2$ and can be even more for the injected ions when their pitch angles correspond to transitioning particles, $v_{||}/v \sim \sqrt{\epsilon_m} \sim 0.3$. However, the diffusion process is relatively slow. Therefore, the diffusion not necessarily leads to the loss of ions of high energy to the wall. When the electron temperature is characterized by strongly peaking radial distribution whereas the electron density profile is flat, the energetic ions will be thermalized near the edge before being lost. A key parameter affecting the magnitude of the diffusion coefficient is the ratio a/ρ_B ($D \propto \omega_B(\rho_B/a)^4$). The diffusion coefficient grows with the plasma pressure ($D \propto \epsilon_0'$). Nevertheless, it can be rather small in the plasma core (where the most of α-particles are produced) even in high-β plasmas provided that ϵ_0' is minimized at $r/a \leq 0.5$. However, we should note that ϵ_0' must exceed a certain magnitude to avoid superbanana orbits.

The estimates for the diffusion time and the fraction of lost particles which follows from our theory agree with the results of numerical modelling carried out in this work and in the earlier works[15,16]. This show that the considered stochastic diffusion is responsible for the loss of energetic ions ($\Delta\mathcal{E} \ll 1$) for $\Delta t \geq 0.02s$ observed in the mentioned numerical experiments.

A general conclusion which follows from our work is that the stochastic diffusion of transitioning particles is an important factor which affects the confinement of energetic particles in optimized stellarators. The dependence of the obtained diffusion coefficient on plasma parameters and relatively large diffusion time (τ_d) indicate that there should exist the optimum profile shapes of the electron density and temperature minimizing the

effect of the stochastic diffusion on the loss of energetic transitioning particles in Helias configurations.

V. ACKNOWLEDGEMENTS

The work is carried out within the Partner Project Agreement No. P-034 between the Science and Technology Center in Ukraine and the Scientific Center "Institute for Nuclear Research", and Max-Planck-Institut für Plasmaphysik. The authors thank and V.V. Lutsenko for the help with graphycal tools. Two of the authors (Ya.K. and V.M.) would like to acknowledge the hospitality of the Max-Planck-Institut für Plasmaphysik.

REFERENCES

[1] S.L. Painter, J.F. Lyon, Fusion Technol. **16**, 157 (1989).

[2] G. Grieger, C. Beidler, E.Harmeyer, et al., in Plasma Phys. Contr. Fusion Res. (Proc. 12th Int. Conf., Nice 1988) Vol. 2, IAEA, Vienna 369 (1989).

[3] C.D. Beidler, G. Grieger, E. Harmeyer, et al., Fusion Energy 1996 (Proc. 16th IAEA Conf., Montreal) IAEA, Vienna, Vol. 3, 407 (1997).

[4] J. Nührenberg, and R. Zille, Phys. Letters A **129** 113 (1988).

[5] J. Nührenberg, W. Lotz, S. Gori, Theory of Fusion Plasmas (Varenna, 1994), Editrice Compositori, Bologna (1994).

[6] P.R.Garabedian, Phys. Plasmas **3**, 2483 (1996).

[7] J.R. Cary, S.G. Shasharina, Phys. Rev. Lett. **78**, 674 (1997).

[8] A.V. Timofeev, Sov. Phys.-JETP **48**, 656 (1978).

[9] J.R. Cary, D.F. Escande, J.L. Tennyson, Phys. Rev. A **34**, 4256 (1986).

[10] A.I. Neishtadt, Sov. J. Plasma Phys. **12**, 992 (1986).

[11] S.V. Putvinskij, B.J.D. Tubbing, L.-G. Eriksson, S.V. Konovalov, Nuclear Fusion **34**, 495 (1994).

[12] M.H. Redi, R.V. Budny, D.S. Darrow, et al., Nuclear Fusion **35**, 1509 (1995).

[13] R.J. Goldston, R.B. White, A.H. Boozer, Phys. Rev. Lett. **47**, 647 (1981).

[14] V.S. Marchenko, Nuclear Fusion **35**, 69 (1995).

[15] W. Lotz, P. Merkel, J. Nührenberg, E. Strumberger, Plasma Phys. Control. Fusion **34** 1037 (1992).

[16] W. Lotz, J. Nührenberg, in "Theory of Fusion Plasmas", Bologna, 17 (1992).

[17] H. Wobig, C.D. Beidler, J. Kisslinger, E. Harmeyer, F. Herrnegger, Fusion Energy 1998

(Proc. 17th IAEA Conference, Yokohama) IAEA **4**, (1999) 1.

[18] L.M. Kovrizhnykh, S.G.Shasharina, Nuclear Fusion **30**, 453 (1990).

[19] A.H. Boozer, Phys. Fluids **24**, 1999 (1981).

[20] R. B. White and M. S. Chance, Phys. Fluids **27**, 2455 (1984).

[21] P.N. Yushmanov, in Reviews of Plasma Physics, vol.16, Consultants Bureau, New York (1990) 55.

[22] G. Grieger, Nucl. Fusion Suppl. **3**, 525 (1991).

FIGURES

FIG. 1. Sketch of level contours of J for the locally trapped particles (thin lines) and the $\kappa = 1$ contour (bold line inside the plasma) in a Helias. Locally trapped particles moving along the $J = \text{const}$ contours become locally passing ones after crossing the bold line.

FIG. 2. Fourier harmonics of the magnetic field strength in a Helias reactor and the high-mirror high-ι variant of Wendelstein 7-X with $\langle\beta\rangle = 4.7\%$.

FIG. 3. Diffusion coefficient versus the pitch parameter $\alpha \equiv \mathcal{E}/\mu B - 1$ for various r/a. The following parameters were used: $\langle\beta\rangle = 4.7\%$, $a/\rho_B = 30$, $B = 4.75T$.

FIG. 4. Radial dependence of the diffusion coefficient and $\alpha_0 = (\alpha_{max} + \alpha_{min})/2$ for the same parameters as in Fig. 3. The used magnitudes of α are shown by the dashed line.

FIG. 5. The diffusion time versus α for the Fourier harmonics of the magnetic field shown in Fig. 2.

FIG. 6. Fraction of transitioning particles versus r for the same parameters as in Fig. 3.

FIG. 7. Density and temperature profiles used for the high-n, low-T (solid line) and low-n, high-T (dotted line) scenarios. Also shown are the corresponding α-particle birth profiles as cumulative probability curves.

FIG. 8. The fraction of initial energy transferred to the background plasma before its escape, $\Delta\mathcal{E}$, is plotted as a function of confinement time, τ_{loss}, (symbol: $\circ$) for each of the 19 α-particles lost during the $0.12\,s$ of the high-n, low-T simulation. Also shown is the normalized radius at which the particle began the simulation, x_0 (symbol: $\square$).

FIG. 9. As in Fig. 8 for the 54 α-particles lost during the $0.44\,s$ of the low-n, high-T simulation.